



Electrodeposition of crack-free and amorphous Ni-Mo alloys with high Mo content from gluconate baths

Eletr deposição de ligas amorfas de Ni-Mo e sem trincas com alto teor de Mo a partir de banhos de gluconato

A. F. Almeida¹; J. D. Costa^{2*}; M. B. Sousa¹; J. I. V. Souto²; R. A. C. Santana²; A.X. Santos³; J. A. M. Oliveira²; J. J. N. Alves¹; A. R. N. Campos¹

¹ Academic Unit of Chemical Engineering, Federal University of Campina Grande, 58429-900, Campina Grande-PB, Brazil

² Academic Unit of Mechanical Engineering, Federal University of Campina Grande, 58429-900, Campina Grande-PB, Brazil

³ Academic Unit of Cabo de Santo Agostinho, Rural Federal University of Pernambuco, 54518-430, Cabo de Santo Agostinho-PE, Brazil

*josianeeq@gmail.com

(Recebido em 25 de abril de 2023; aceito em 02 de outubro de 2023)

In this article, electroplated Ni-Mo alloys with high Mo content from gluconate baths are presented. Specifically, the influence of current density on the electrodeposition process, which produced crack-free Ni-Mo alloys with high Mo content, was evaluated. Commonly, Ni-Mo electrodeposition is performed in citrate solutions, as citrate ions promote coordination compounds with greater stability compared to mono and bivalent ligands. However, due to the high internal stress caused by Mo in the coating when its content is very high, microcracks are formed along the surface, causing defects in the deposit. Gluconate baths have been proven to produce crack-free alloys, even when current density is high. The deposits were evaluated for chemical composition by Energy-Dispersive X-ray Spectrometry (EDS) and surface morphology by electron microscopy using a Scanning Electron Microscope (SEM). Furthermore, the deposition process was evaluated for current efficiency, and a reaction mechanism was proposed based on observations acquired by other authors. The highest Mo content obtained was 43% by weight. The highest current efficiency was 26%, obtained at 30 mA/cm².

Keywords: electrodeposition, Ni-Mo, sodium gluconate.

Neste artigo, são apresentadas ligas de Ni-Mo eletrodepositadas com alto teor de Mo a partir de banhos de gluconato. Especificamente, foi avaliada a influência da densidade de corrente no processo de eletrodeposição, que produziu ligas de Ni-Mo sem trincas com alto teor de Mo. Comumente, a eletrodeposição de Ni-Mo é realizada em soluções de citrato, pois os íons de citrato promovem compostos de coordenação com maior estabilidade em comparação com ligantes mono e bivalentes. No entanto, devido ao alto estresse interno causado pelo Mo no revestimento quando seu teor é muito alto, microtrincas são formadas ao longo da superfície, causando defeitos no depósito. Banhos de gluconato foram comprovados para produzir ligas sem trincas, mesmo quando a densidade de corrente é alta. Os depósitos foram avaliados quanto à composição química por EDS e à morfologia superficial por SEM. Além disso, o processo de deposição foi avaliado quanto à eficiência de corrente, e um mecanismo de reação foi proposto com base em observações adquiridas por outros autores. O maior teor de Mo obtido foi de 43% em peso. A maior eficiência de corrente foi de 26%, obtida a 30 mA/cm².

Palavras-chave: eletrodeposição, Ni-Mo, gluconato de sódio.

1. INTRODUCTION

Ni-Mo alloys are well known for their remarkable properties of high corrosion and wear resistance [1, 2], elevated electrocatalytic activity [3], and low thermal expansion coefficient [4]. Their possible applications include catalyst-support coatings [5] and microelectronic devices [6]. It is well known that Mo requires the presence of another metal (generally those from group 8 B) and a complexing agent in the electrolyte because the electrodeposition of Mo is governed by induced co-deposition [7]. Typically, such complexing agents are organic compounds with pairs of electrons available for coordination. Indeed, the current efficiency of electrodeposition of Ni-Mo films tends to be elevated in the presence of sodium citrate. For example, Santana et al.

(2010) [8] found a current efficiency of 92%, characteristic of coatings with high Ni contents. In contrast, when the Mo content increases, the efficiency tends to drop because of the higher nucleation rate as current density increases, for example [9]. Increasing the content of Mo in the deposit is interesting. However, it shows some consequences in the surface morphology of the coatings: as the atomic radius of Mo is greater than the Ni's, the formation of microcracks is practically inevitable, diminishing the capacity of the films to be employed in aggressive corrosive mediums, as such cracks are responsible for localized oxidation [10-12].

Even though citrate baths tend to be reasonably stable for Ni-Mo electrodeposition and using less stable complexing agents might not be recommended, there are examples where such complexing agents have been used. In a previous study, we investigated the influence of bath chemistry on the electrodeposition of Ni-Mo alloys from tartrate baths in acidic media [13]. Other films can also be obtained using mono- or bi-valent ligands. Rudnik and Włoch (2014) [14] investigated the influence of sodium gluconate ($NaC_6H_{11}O_7$) on the electrodeposition process of Ni-Mn films. Ma et al. (2017) [15] investigated the effect of current density, temperature, and pH on the properties of the coatings. Although the gluconate ion is a monovalent ligand in complexation reactions [16], coatings can be produced at considerable current efficiencies, depending on the bath and operational parameters. Bera et al. (2013) [17] observed current efficiency in the 62 – 70% range when investigating Co-W electrodeposition in gluconate baths. Weston et al. (2010) [18] observed close to 50% current efficiencies in Co-W electrodeposition. Mahalingam and Bera (2021) [19] found remarkable current efficiencies in the 40 – 79% range. Some alloys have already been obtained from gluconate baths; however, to our knowledge, there are only a few reports on producing Ni-Mo alloys from such electrolytes [20]. In their study, the authors used salts containing Ni and Mo in baths with sulfamate content and additives such as saccharin and sodium lauryl sulfate. They obtained Ni-Mo coatings using high-current-efficiency electrodeposition processes, which the Ni can explain:Mo ratio of 100:1 g/L.

As can be seen, the chemistry of the bath is fundamental in the electrodeposition process, especially in the case of additives that participate in complexation reactions, which may or may not be mandatory to acquire suitable Ni-Mo coatings. Other aspects must be considered. In this way, investigators usually evaluate the influence of operating variables such as the applied current density and temperature, which may vary according to the coatings [21]. In general, the role of each of these variables is well-known. The potential applied acts as an electromotive force for the phenomena to occur; it is responsible for attracting metallic cations to the negatively polarized surface (cathode), where they can be electrochemically reduced. Consequently, current emerges within the system, imposing current lines, which are responsible for the conducting ion migration phenomena. In turn, the temperature can modify the ionic mobility so that the cations may be easily driven to the cathode [22]; one should be careful when increasing the temperature to avoid degrading the coordination compounds formed.

Regarding the Ni-Mo-based coatings, the current density was set in different ranges depending on the desirable morphology. For instance, Shetty et al. (2017) [23] conducted their experiments in the range of 10 mA/cm^2 – 40 mA/cm^2 to obtain crystalline Ni-Mo deposits with 33.2 Mo wt.%. Li et al. (2021) [24] employed 50 mA/cm^2 in a pulsed electrodeposition methodology and found deposits with a diverse region of amorphous and nanocrystalline solids. In a previous paper, we developed amorphous Ni-Mo by conducting experiments at 60 mA/cm^2 [25]. The authors found their results by setting the temperature at 30 °C [21], –20 °C [22], and 70 °C (our previous paper). There is no direct and well-defined temperature profile, indicating a clear transition between crystallinity and amorphous solids because it depends on other variables, especially the bath chemistry associated with controllable parameters such as agitation and current density.

Therefore, not only is the bath chemistry of the bath important for understanding how electrochemical reduction occurs, but also how the operating variables act during the process. Hence, to investigate the electrodeposition of Ni-Mo alloys from gluconate baths, this paper presents the initial steps of how the current density affects the chemical composition of the coatings and their morphologies from baths containing a high Ni:Mo concentration ratio. The results show that no cracks were formed even when the Mo content was elevated, which is present in Ni-Mo coatings obtained from citrate baths. For characterization purposes, the chemical

composition of the alloys were obtained by EDX analysis and surface morphology results by SEM. Finally, the electrodeposition process was evaluated in terms of the current efficiency.

2. MATERIALS AND METHODS

2.1 Electrodeposition

Galvanostatic electrodeposition of Ni-Mo alloys was conducted in a two-electrode cell with a PGSTATE302N Autolab connected to NOVA 2.1.4. The working electrode was a copper foil of 8 cm² of total active area, and the counter electrode was a mesh Pt gauze with 112 cm² of total active area. Before each deposition, the substrates were treated mechanically and chemically. The former involved polishing the electrode surface with 320–1200 grit silicon carbide papers to minimize surface irregularities. For the latter, the copper electrodes were submerged in H₂SO₄ 1% (V/V) and NaOH 10% (m/V). Chemical treatments focus on cleansing and removing possible oxides. The electrolyte was prepared with reagents of high purity degree: C₆H₁₁NaO₇ (Neon, 99.48%) 0.2 mol/L, NiSO₄·6H₂O (Neon, 98.18%) 0.053 mol/L, and Na₂MoO₄·2H₂O (Neon, 99.64%) 0.050 mol/L. The concentrations were chosen according to the work of Weston et al. (2010) for Co-W electrodeposition [18]. The current densities applied to this study were 30 mA/cm², 45 mA/cm², and 60 mA/cm². The temperature was kept constant at 75 °C with a thermostatic bath novatecnica NT246; pH was adjusted to 6.0 with a pHmeter Quimis Q400R by adding NaOH 50% (m/V) and H₂SO₄ 50% (V/V), when necessary. All experiments were performed under quiescent conditions. The electric charge for each experiment was 600 C. All experiments were performed in duplicate.

2.2 Chemical Composition and Current Efficiency

Energy-Dispersive X-ray Spectroscopy performed chemical composition measurements with a spectrometer Shimadzu EDX-720. In addition, current efficiency was analyzed by Faraday's law using the equation expressed in a previous study [25].

2.3 Surface morphology and microstructure analyzes

The surface morphology was evaluated using Scanning Electron Microscopy (SEM) and Energy-Dispersive Spectroscopy (EDS) for microscopic superficial images and surface mapping, respectively, using a Tescan Oxford microscope. The microstructure of the coatings was analyzed by X-ray Diffraction (XRD), which was conducted with an X-ray diffractometer Shimadzu 6100 with scanning range from 30° to 60°, K α target of 15.4 nm wavelength at 30 kV and 30 mA, step size of 0.02°, and dwell time of 1 second.

3. RESULTS AND DISCUSSION

3.1 Chemical composition and current efficiency

The influence of current density on the electrodeposition process of Ni-Mo alloys in the presence of sodium gluconate was investigated. Prior to the depositions, preliminary tests indicated that the deposition was impossible for temperatures (T) below 70°C at pH 6. This contrasts with what was observed by other investigators that employed similar conditions (bath chemistry and operational parameters) for the study of thin films as Co-W [26, 27]. Similar observations were expected because Co is intrinsically related to Ni, as they are both parts of group 8 B, and W is intrinsically related to Mo for the same reason as Co and Ni. The Co-W coatings produced from gluconate baths present good properties owing to their high W content,

and the applied current is used effectively to reduce Co and W electrochemically; that is, the electrodeposition process is conducted at a high current efficiency. For example, Yar-Mukhamedova et al. (2018) [28] developed crack-free Co-W coatings with at.% W equals to 18.4, and more than 72% of current efficiency. However, for $T < 70^{\circ}\text{C}$, the coatings did not adhere to the substrate as expected, being easily removed with emery paper of 1200 grit; increasing T to 75°C partially solved the problem and the Ni-Mo coatings produced were with good adhesion to the Cu substrate.

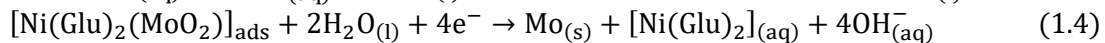
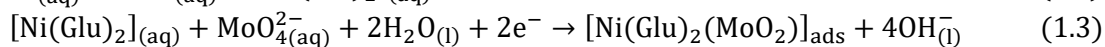
For current densities below 30 mA/cm^2 , lack of adherence was observed; low current densities did not promote the deposition of Mo in high quantities. Therefore, a large amount of nickel was reduced on the cathode, resulting in a scaly appearance and remarkably low adhesion. It is noteworthy that the current density controls the chemical composition, microstructure of the alloys, electrodeposition rate, and cathodic current efficiency [29], which was considered the minimum required for the electrodeposition process of Ni-Mo films investigated in this study. Therefore, the experiments were conducted in an acidic medium ($\text{pH} = 6.0$), at $T = 75^{\circ}\text{C}$, with current density varying from 30 mA/cm^2 to 60 mA/cm^2 . Table 1 shows the chemical composition of all deposits obtained. All experiments were performed in duplicates. The chemical composition results presented correspond to the arithmetic mean of the chemical compositions, and standard deviation values are shown.

Table 1 – Results of chemical composition, current efficiency, and corrosion properties.

Exp	J(mA/cm^2)	Mo content (wt. %)	Thickness (μm)	CE(%)
1	30	Ni61Mo(39 ± 0.04)	1.532	26.11
2	45	Ni59Mo(41 ± 0.05)	0.473	7.28
3	60	Ni57Mo(43 ± 0.08)	0.386	4.42

J: current density; CC: experimental chemical composition; SD: standard deviation; CE: current efficiency.

Table 1 shows that the Mo content increased as the current density increased up to 60 mA/cm^2 in experiment 3. According to Bigos et al. (2017) [30], when increasing the factors that accelerate the mass transport of metal ions cause an increase in the content of the refractory metal in the alloy (Mo in this case); one can conclude that diffusion limits Mo deposition. Not surprisingly, in the literature, this conclusion relates to the electrodeposition of Ni-Mo in citrate baths as it is the most used complexing agent in Ni-Mo electrodepositions, which follows the mechanism established by Podlaha and Landolt (1996) [31]. Table 1 also suggests that this pattern is followed in the present case so that the Mo content varies with the current density in gluconate baths like in citrate solutions. However, for current densities higher than 60 mA/cm^2 , Ni^{2+} reduction is preferable, and the Mo content drops. Such observation can be associated with the poor stability of the coordination compounds formed between gluconate and Ni^{2+} ions, which precludes the Mo deposition. Hence, as the Mo content increases with current density, it is suggested that the mechanism for the Mo reduction reaction in co-deposition with Ni in gluconate baths follows the same pattern as that with citrate ions proposed by Podlaha and Landolt, which was later confirmed by Zeng et al. (2000) [32]. A reasonable mechanism for the electrodeposition of Ni-Mo alloys using sodium gluconate as a complexing agent is proposed and described by Equations 1.1 – 1.6, as follows:



The current density affects the cathodic efficiency of the process. As the current density and the Mo content increased, the current efficiency decreased significantly. This observation is related to the fact that Mo deposition is essentially controlled by mass transfer [33], whereas Ni reduction is kinetically driven [34]. Therefore, by increasing the current density, the voltage between the working electrode and the counter electrode increased, favoring the transport of $[\text{NiGlu}_2]$ complexes to the surface of the cathode. However, the formation of gas on the surface of the cathode favors an increase in the Mo content in the alloy [31], which occurs because Ni-Mo alloys are extremely electrocatalytic [26, 35-37]. As a result, when increasing the current density, the hydrogen retained on the cathode surface is more easily reduced to H_2 and released to the atmosphere, promoting the reduction of metals onto the cathode and, consequently, producing alloys with higher Mo contents, which justifies the considerable drop in current efficiency results.

Such behavior was observed for current densities up to 60 mA/cm^2 , from which a substantial decay was observed in the Mo content. When the production of H_2 increases on the surface of the working electrode, most of the energy used in the electrodeposition process is diverted for hydrogen evolution purposes [36] at a higher rate, which inhibits the diffusion of ionic species of Mo as the applied current density is used for HER and not for electrochemical reduction of Mo. The main reason for the substantial decline in current efficiency, even though the current density was increased.

3.2 Surface morphology and microstructure analyses

Figure 2 presents the SEM micrographs of the alloys obtained from experiments 1 to 3. From these images, it can be seen that the current density has a significant influence on the surface morphology of the obtained alloys. For 30 mA/cm^2 , the alloy presented a smaller number of nodules, but more expressive. This characteristic is a consequence of the large amount of Ni in the coating, as evidenced by the chemical composition results. With an increase in the current density, smaller nodules were observed, which is a direct consequence of the increase in the nucleation rate. It is highlighted that there were no apparent microcracks along the surface of any film obtained in this study. According to Chassaing et al. (2004) [38], alloys with molybdenum contents higher than 30 wt. % present cracks due to high internal stress in the deposit. However, in the present work, it was possible to obtain alloys with Mo contents of approximately 40 wt. % without any sign of cracks. Figure 1A represents the surface microscopy for the NiMo39 alloy.

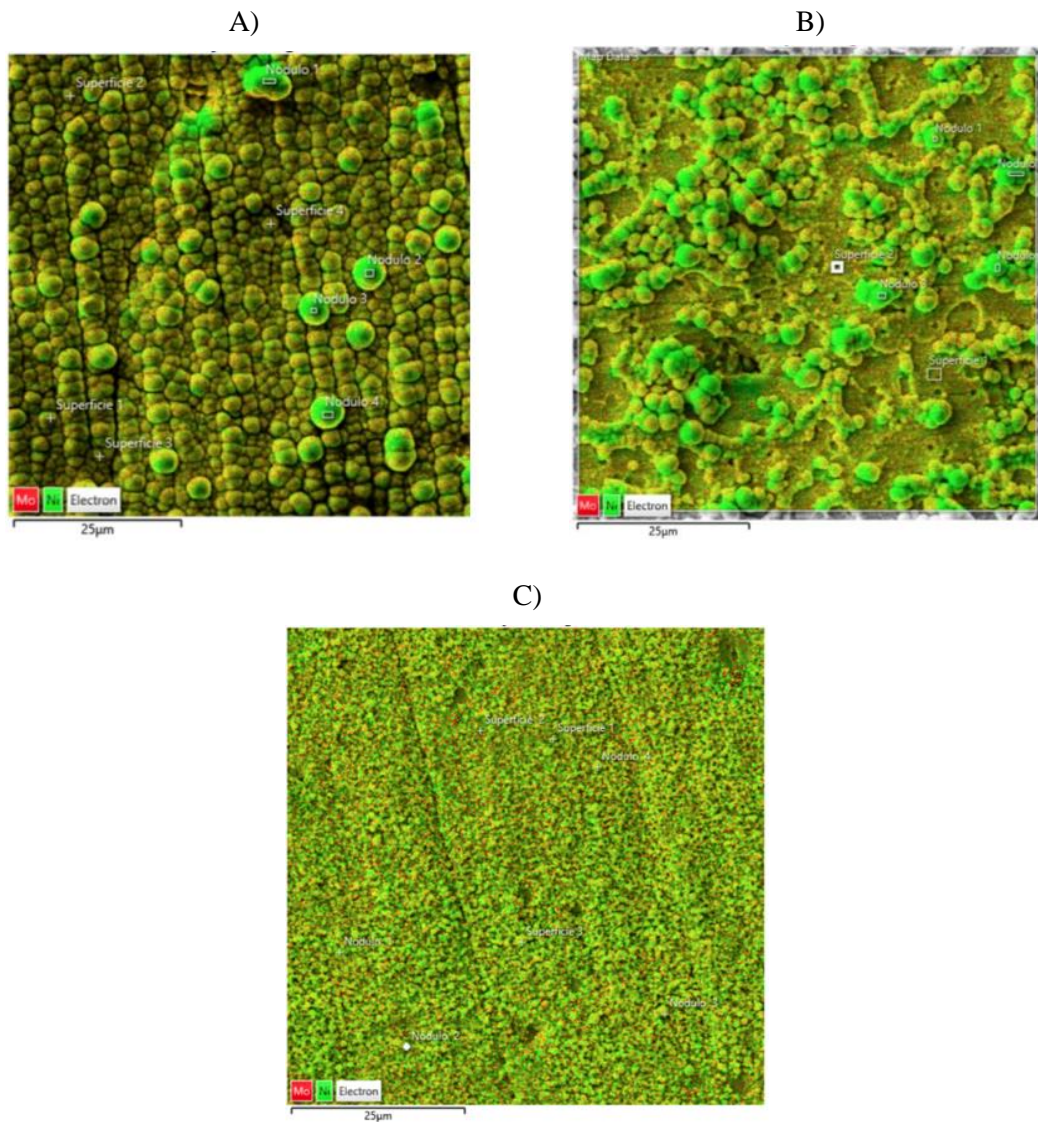


Figure 1 – Surface morphology and element distribution throughout the surfaces of the deposits of the alloys obtained at A) 30 mA/cm² - NiMo39, B) 45 mA/cm² NiMo41, and C) 60 mA/cm² - NiMo43.

To assess the influence of current density on the alloy structure, XRD analyzes were performed. Figure 2 shows the diffractograms for copper samples coated with Ni-Mo alloys obtained in each experiment according to the molybdenum content.

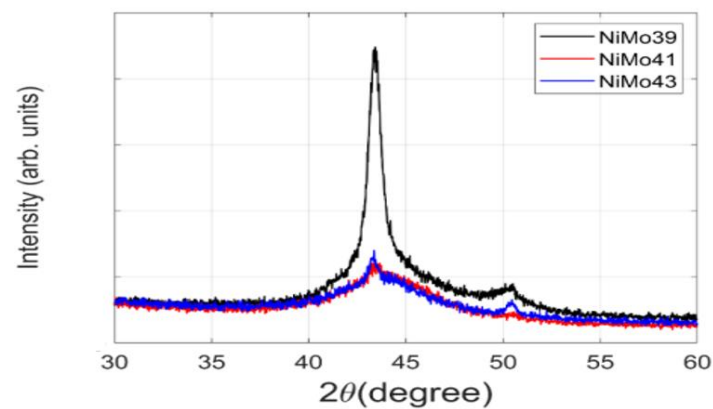


Figure 2 – Diffractograms for the coatings NiMo39 (exp 1), NiMo41 (exp 2) and NiMo43 (exp 3).

According to Surani Yancheshmeh and Ghorbani (2014) [39], the alloys' surface morphology and microstructure strongly depend on their molybdenum composition. In their work, the authors stated that the deposition of Ni is limited due to the decreased mobility of Ni atoms in the structure of the Ni-Mo alloy. They declare it is explained by the difficulty of Ni diffusion due to the reduction of empty spaces in the crystalline network, also occupied by Mo atoms by the induced co-deposition process, giving the alloy an amorphous characteristic.

Figure 2 shows that for Ni-Mo alloys with 39 wt.% Mo content (exp 1), characteristic peaks of the alloy around 43° are widened. When the Mo content increased from 39 to 41 wt. % (exp 2), the peaks' further widening and considerable drop in their intensity are observed. Studies in the literature confirm such results when they mention that for high levels of molybdenum in the alloy, the material passes from crystalline to nanocrystalline/amorphous [40-42].

Although the Mo contents are remarkably close to each other in the presented alloys, it is observed that an increase in the current density also increases the Mo content. Huang et al. (2014) [43] obtained similar results regarding the proximity of the chemical composition and, even so, differences in the diffractograms presented.

By increasing the current density from 45 mA/cm² (exp 2) to 60 mA/cm² (exp 3), the Mo content in the alloy increased from 41 wt.% (exp 2) to 43 wt.% (exp 3). Consequently, the diffractogram showed peaks with more expressive intensities. As the coating with Mo 43 wt.% was very thin, the peaks observed in the diffractogram are characteristic of copper overlapping those of the Ni-Mo alloy, which is also around 43° [39].

4. CONCLUSION

The results obtained in this study indicate that it is possible to obtain crack-free Ni-Mo alloys with a high Mo content using sodium gluconate as a complexing agent. Even at acidic pH, the obtained alloys showed good adhesion to the substrate. The effect of current density was observed to be significant in the analysis of the composition deposit chemistry and in the microstructure and cathodic efficiency of the alloys obtained. With an increase in density, there was a decrease in the nickel content in the alloys and, consequently, an increase in the Mo content. The current density also influenced the microstructure of the alloy. A more significant amount of Mo was observed in the alloy with smaller nodules at higher current densities. No microcracks were observed during the electrodeposition of Ni-Mo in citrate baths. Hence, sodium gluconate has proven to be an excellent complexing agent for obtaining Ni-Mo alloys via electrodeposition. It is an alternative to citrate electrolytes, as the deposition produces deposit coatings with high Mo content without cracks, with experiments showing good current efficiency.

5. ACKNOWLEDGEMENTS

This study was financed in part by the Coordenação de Aperfeiçoamento de Pessoal de Nível Superior – Brasil (CAPES) – Finance Code 001. We are grateful to the Conselho Nacional de Desenvolvimento Científico e Tecnológico (CNPq) for granting a scholarship on Productivity in Technological Development and Innovative Extension–DT Level 2 (Grant #308251/2020-2). We are grateful to the Laboratory of Microscopy of the Department of Mechanical Engineering (Federal University of Campina Grande) for technical support.

6. REFERENCES

1. Bigos A, Janusz-Skuza M, Szczerba MJ, Kot M, Zimowski S, Dębski A, et al. The effect of heat treatment on the microstructural changes in electrodeposited Ni-Mo coatings. *J Mater Process Technol.* 2020 Feb;276:116397. doi: 10.1016/j.jmatprotec.2019.116397

2. Liu JH, Li WH, Pei ZL, Gong J, Sun C. Investigations on the structure and properties of nanocrystalline Ni-Mo alloy coatings. *Mater Charact.* 2020 Sep;167:110532. doi: 10.1016/j.matchar.2020.110532
3. Bau JA, Kozlov SM, Azofra LM, Ould-Chikh S, Emwas A-H, Idriss H, et al. Role of oxidized Mo Species on the active surface of Ni-Mo electrocatalysts for hydrogen evolution under alkaline conditions. *ACS Catal.* 2020 Oct;10(21):12858-66. doi: 10.1021/acscatal.0c02743
4. Han L, Jeurgens LPH, Cancellieri C, Wang J, Xu Y, Huang Y, Liu Y, Wang Z. Anomalous texture development induced by grain yielding anisotropy in Ni and Ni-Mo alloys. *Acta Mater.* 2020 Nov;200:857-868. doi: 10.1016/j.actamat.2020.09.063
5. Vahid S, Mirzaei AA. An investigation of the kinetics and mechanism of Fischer-Tropsch synthesis on Fe-Co-Ni supported catalyst. *J Ind Eng Chem.* 2014 Jul;20(4):2166-73. doi: 10.1016/j.jiec.2013.09.047
6. Tang J, Zhao X, Zuo Y, Ju P, Tang Y. Electrodeposited Pd-Ni-Mo film as a cathode material for hydrogen evolution reaction. *Electrochim Acta.* 2015 Aug;174:1041-9. doi: 10.1016/j.electacta.2015.06.134
7. Brenner A. Electrodeposition of alloys: Principles and practice. Vol. II, first edit. Washington (US): Elsevier; 1963. doi: 10.1016/C2013-0-07892-9
8. Santana RAC, Casciano PNS, Oliveira ALM, Nascimento IO, Silva TFT. Otimização dos constituintes do banho eletrolítico da liga Ni-Mo obtida por eletrodeposição, *Rev Eletr Mater Processos.* 2010 Jul;5(2):1-11.
9. Rashtchi H, Raeissi K, Shamanian M, Acevedo Gomez Y, Lagergren C, Wreland Lindström R, et al. Evaluation of Ni-Mo and Ni-Mo-P electroplated coatings on stainless steel for PEM fuel cells bipolar plates. *Fuel Cells.* 2016 Oct;16(6):784-800. doi: 10.1002/fuce.201600062
10. Liu H, Liu Z. Evaluation of microstructures and properties of laser-annealed electroless Ni-P/Ni-Mo-P duplex coatings. *Surf Coat Technol.* 2017 Dec;330:270-6. doi: 10.1016/j.surfcoat.2017.10.012
11. He FJ, Fang YZ, Jin SJ. The study of corrosion-wear mechanism of Ni-W-P alloy. *Wear.* 2014 Mar;311(1-2):14-20 doi: 10.1016/j.wear.2013.12.024
12. Polo JL, Cano E, Bastidas JM. An impedance study on the influence of molybdenum in stainless steel pitting corrosion. *J Electroanal Chem.* 2002 Nov;537(1-2):183-7. doi: 10.1016/S0022-0728(02)01224-X
13. Filgueira de Almeida A, Costa Neto H, Santana RAC, Alves JN, Nascimento Campos AR, Prasad S. Influence of bath composition on the electrodeposition of amorphous Ni-Mo alloys using potassium-sodium tartrate as complexing agent. *Can J Chem Eng.* 2021 Jan;99:S284-94. doi: 10.1002/cjce.24043
14. Rudnik E, Włoch G. The influence of sodium gluconate on nickel and manganese codeposition from acidic chloride-sulfate baths. *Ionics (Kiel).* 2014 May;20:1747-55. doi: 10.1007/s11581-014-1137-9
15. Ma L, Xi X, Nie Z, Dong T, Mao Y. Electrodeposition and characterization of Co-W alloy from regenerated tungsten salt. *Int J Electrochem Sci.* 2017 Dec;12:1034-51. doi: 10.20964/2017.02.37
16. Kutus B, Dudás C, Orbán E, Lupan A, Attia AAA, Pálinkó I, et al. Magnesium(II) d-Gluconate complexes relevant to radioactive waste disposals: Metal-ion-induced ligand deprotonation or ligand-promoted metal-ion hydrolysis?. *Inorg Chem.* 2019 May;58:6832-44. doi: 10.1021/acs.inorgchem.9b00289
17. Bera P, Seenivasan H, Rajam KS, Shivakumara C, Parida SK. Characterization and microhardness of Co-W coatings electrodeposited at different pH using gluconate bath: A comparative study. *Surf Interface Anal.* 2013 Jan;45:1026-36. doi: 10.1002/sia.5209
18. Weston DP, Harris SJ, Shipway PH, Weston NJ, Yap GN. Establishing relationships between bath chemistry, electrodeposition and microstructure of Co-W alloy coatings produced from a gluconate bath. *Electrochim Acta.* 2010 Aug;55(20):5695-708. doi: 10.1016/j.electacta.2010.05.005
19. Mahalingam DK, Bera P. Characterization and microhardness of Ni-W-P coatings electrodeposited with gluconate bath. *Surf Interfaces.* 2021 Feb;22:100769. doi: 10.1016/j.surfin.2020.100769
20. Matsui I, Omura N, Li M, Murakami Y, Tada S. Fabrication of electrodeposited bulk nanocrystalline Ni-Mo alloys from a gluconate bath and their mechanical properties. *Surf Technol.* 2016;67(8):434-9. doi: 10.4139/SFJ.67.434
21. Gupta A, Srivastava C. Electrodeposition current density induced texture and grain boundary engineering in Sn coatings for enhanced corrosion resistance. *Corros Sci.* 2022;194:109945. doi: 10.1016/j.corsci.2021.109945
22. You H, Yang P, Wang X, Yang X, Sun Y, An M. Electrodeposition of nanocrystalline Ni-Mo alloys in pyrophosphate baths. *J Alloys Compd.* 2022;924:166407. doi: 10.1016/j.jallcom.2022.166407
23. Shetty S, Mohamed JSM, Bhat DK, Hegde AC. Electrodeposition and characterization of Ni-Mo alloy as an electrocatalyst for alkaline water electrolysis. *J Electroanal Chem.* 2017 Jul;796:57-65. doi: 10.1016/j.jelechem.2017.05.002

24. Li J, Shi Y, Li X. Pulse electrodeposited Ni-26 at. %Mo—A crossover from nanocrystalline to amorphous. *Nanomater.* 2021 Mar;11(3):681. doi: 10.3390/nano11030681
25. Almeida AF, Souto JIV, Santos ML, Santana RAC, Alves JJJ, Campos ARN, et al. Establishing relationships between bath composition and the properties of amorphous Ni–Mo alloys obtained by electrodeposition. *J Alloys Compd.* 2021 Dec;888:161595. doi: 10.1016/j.jallcom.2021.161595
26. Abuin G, Coppola R, Diaz L. Ni-Mo alloy electrodeposited over Ni substrate for HER on water electrolysis. *Electrocatalysis.* 2018 Sep;10:17-28 doi: 10.1007/s12678-018-0490-2
27. Gotelyak AV, Silkin SA, Yakhova EA, Dikumar AI. Effect of pH and volume current density on deposition rate and microhardness of Co–W coatings electrodeposited from concentrated boron–gluconate electrolyte. *Russ J Appl Chem.* 2017 Jul;90:541-6. doi: 10.1134/S1070427217040085
28. Yar-Mukhamedova G, Ved' M, Sakhnenko N, Nenastina T. Electrodeposition and properties of binary and ternary cobalt alloys with molybdenum and tungsten. *Appl Surf Sci.* 2018 Jul;445:298-307. doi: 10.1016/j.apsusc.2018.03.171
29. Beltowska-Lehman E, Bigos A, Indyka P, Kot M. Electrodeposition and characterisation of nanocrystalline Ni-Mo coatings. *Surf Coat Technol.* 2012 Oct;211:67-71. doi: 10.1016/j.surfcoat.2011.10.011
30. Bigos A, Beltowska-Lehman E, Kot M. Studies on electrochemical deposition and physicochemical properties of nanocrystalline Ni-Mo alloys. *Surf Coat Technol.* 2017 May;317:103-9. doi: 10.1016/j.surfcoat.2017.03.036
31. Podlaha EJ, Landolt D. Induced codeposition I. An experimental investigation of Ni-Mo alloys. *J Electrochem Soc.* 1996 Mar;143(3):885-92. doi: 10.1149/1.1836553
32. Zeng Y, Li Z, Ma M, Zhou S. In situ surface Raman study of the induced codeposition mechanism of Ni–Mo alloys. *Electrochem Commun.* 2000 Jan;2(1):36-8. doi: 10.1016/S1388-2481(99)00137-X
33. Costovici S, Manea AC, Visan T, Anicai L. Investigation of Ni-Mo and Co-Mo alloys electrodeposition involving choline chloride based ionic liquids. *Electrochim Acta.* 2016 Jul;207:97-111. doi: 10.1016/j.electacta.2016.04.173
34. Jović BM, Jović VD, Maksimović VM, Pavlović MG. Characterization of electrodeposited powders of the system Ni–Mo–O. *Electrochim Acta.* 2008 May;53:4796-804. doi: 10.1016/j.electacta.2008.02.004
35. Hassan HB, Abdel Hamid Z. The electrocatalytic behavior of electrodeposited Ni-Mo-P alloy films towards ethanol electrooxidation. *Surf Interface Anal.* 2013 Feb;45(7):1135-43. doi: 10.1002/sia.5239
36. Mitov M, Chorbadzhyska E, Nalbandian L, Hubenova Y. Nickel-based electrodeposits as potential cathode catalysts for hydrogen production by microbial electrolysis. *J Power Sources.* 2017 Jul;356:467-72. doi: 10.1016/j.jpowsour.2017.02.066
37. Xia M, Lei T, Lv N, Li N. Synthesis and electrocatalytic hydrogen evolution performance of Ni-Mo-Cu alloy coating electrode. *Int J Hydrogen Energy.* 2014 Mar;39(10):4794-802. doi: 10.1016/j.ijhydene.2014.01.091
38. Chassaing E, Portail N, Levy AF, Wang G. Characterisation of electrodeposited nanocrystalline Ni-Mo alloys. *J Appl Electrochem.* 2004 Nov;34:1085-91. doi: 10.1007/s10800-004-2460-z
39. Surani Yancheshmeh H, Ghorbani M. Characterization of pulse reverse Ni–Mo coatings on Cu substrate. *Surf Coat Technol.* 2014 Jan;238:158-64. doi: 10.1016/j.surfcoat.2013.10.065
40. Bigos A, Beltowska-Lehman E, Kot M. Studies on electrochemical deposition and physicochemical properties of nanocrystalline Ni-Mo alloys. *Surf Coat Technol.* 2017 May;317:103-9. doi: 10.1016/j.surfcoat.2017.03.036.
41. Chassaing E, Quang KV. Properties of electrodeposited Ni — Mo alloy coatings. *Surf Coat Technol.* 1992 May;53:257-65.
42. Yar-Mukhamedova G, Ved M, Sakhnenko N, Karakurkchi A, Yermolenko I. Iron binary and ternary coatings with molybdenum and tungsten. *Appl Surf Sci.* 2016 Oct;383:346-52. doi: 10.1016/j.apsusc.2016.04.046
43. Huang PC, Hou KH, Sheu HH, Ger MD, Wang GL. Wear properties of Ni–Mo coatings produced by pulse electroforming *Surf Coat Technol.* 2014 Nov;258:639-45. doi: 10.1016/j.surfcoat.2014.08.024